



NUMERICAL INVESTIGATION OF BUOYANCY DRIVEN HEAT TRANSFER OF WATER-BASED CuO NANOFLUIDS IN A RECTANGULAR ENCLOSURE WITH AN OFFCENTER SOLID CONDUCTING BODY

Çiğdem SUSANTEZ* and Kamil KAHVECİ*

*Trakya University Engineering Faculty Mechanical Engineering Department
22030 Edirne, cigdemsusantez@trakya.edu.tr, kamilk@trakya.edu.tr

(Geliş Tarihi: 17.10.2016, Kabul Tarihi: 01.03.2017)

Abstract: In this study, buoyancy driven heat transfer of water-based CuO nanofluid in a rectangular enclosure with a solid cylinder was investigated numerically for different values of aspect ratio, location and diameter of solid cylinder, solid volume fraction and Rayleigh number. While bottom and upper walls of enclosure are adiabatic, sidewalls are isothermal. Thermal conductivity of solid cylinder was assumed to be equal to that of the base fluid. Governing equations were solved numerically by Comsol Multiphysics finite element modeling and simulation software. Results show that heat transfer rate increases considerably with an increase in the Rayleigh number and solid volume fraction and with a decrease in the solid cylinder diameter. Results also show that heat transfer rate shows an increase with an increase of aspect ratio for low values of Rayleigh number. Finally, results show that heat transfer rate gets its highest value for square enclosure case for high values of Rayleigh number.

Keywords: Nanofluid, Enclosure, Convective heat transfer, Rayleigh number, Nusselt number

MERKEZ DIŞI KATI İLETKEN BİR CİSİM İÇEREN DİKDÖRTGEN KAPALI BİR ORTAMDA SU BAZLI CuO NANOAKIŞKANLAR İÇİN KALDIRMA KUVVETİ ETKİLİ ISI TRANSFERİNİN NÜMERİK İNCELENMESİ

Özet: Bu çalışmada, katı bir silindir içeren dikdörtgenel kapalı bir ortamda su bazlı CuO nanoakışkanlar için kaldırma kuvveti etkili ısı transferi farklı yükseklik genişlik oranı, katı silindirin yeri ve çapı, nanoparçacık hacim oranı ve Rayleigh sayısı değerleri için nümerik olarak incelenmiştir. Kapalı ortamın alt ve üst duvarları adyabatik iken, yan duvarları izotermaldir. Silindirin ısı iletim katsayısının baz akışkaninkine eşit olduğu varsayılmıştır. Yönetici denklemler Comsol Multiphysics sonlu eleman modelleme ve simülasyon yazılımı kullanılarak nümerik olarak çözülmüştür. Sonuçlar, ısı transferinin Rayleigh sayısı ve nanoparçacık hacim oranının artışı ve katı silindir çapının düşüşü ile önemli ölçüde arttığını göstermiştir. Sonuçlar aynı zamanda Rayleigh sayısının düşük değerleri için ısı transferinin yükseklik genişlik oranının artışı ile arttığını göstermiştir. Sonuçlar ayrıca ısı transferinin en yüksek değerlerini Rayleigh sayısının yüksek değerleri ve karesel kapalı ortam durumu için aldığını göstermiştir.

Anahtar Kelimeler: Nanoakışkan, Kapalı ortam, Taşınım ile ısı transferi, Rayleigh sayısı, Nusselt sayısı

NOMENCLATURE

ar : aspect ratio [$ar = H/L$]

c_p : specific heat at constant pressure [$Jkg^{-1}K^{-1}$]

D : diameter of the solid cylinder [m]

g : gravitational acceleration [ms^{-2}]

H : height of the enclosure [m]

k : thermal conductivity [WmK^{-1}]

k^* : ratio of the thermal conductivity of the solid cylinder to that of the base fluid

L : width of the enclosure [m]

Nu : Nusselt number [$-\frac{k_{eff}}{k_f} \frac{\partial T^*}{\partial x^*} \Big|_{x^*=0}$]

n : shape factor [$= 3/\Psi$]

\vec{n} : unit normal vector

P : pressure [Pa]

Pr : Prandtl number [$= \frac{\nu_f}{\alpha_f}$]

\dot{q} : heat flux [Wm^{-2}]

Ra : Rayleigh number [$= \frac{g\beta_{T,f}L^3\Delta T}{\nu_f\alpha_f}$]

T : temperature [K]

u : velocity component in x direction [ms^{-1}]

v : velocity component in y direction [ms^{-1}]

x : horizontal coordinate [m]

y : vertical coordinate [m]

Greek symbols

α : thermal diffusivity [m^2s^{-1}]

β : ratio of the liquid nanolayer thickness to the original particle radius

β_T : thermal expansion coefficient [K^{-1}]

ΔT : temperature difference [K]

μ : dynamic viscosity [Pa s]

ν : kinematic viscosity [m^2s^{-1}]

ϕ : solid volume fraction
 Ψ : sphericity
 ρ : density [kgm^{-3}]

Subscripts

a: average
c: cylinder
C: cold
eff: effective
f: fluid
H: hot
S: surface
s: solid
1: outside of the solid cylinder
2: inside of the solid cylinder

Superscripts

*: dimensionless variable

INTRODUCTION

Conventional heat transfer fluids have relatively low thermal conductivity and this is the main drawback in enhancing the heat transfer performance of many engineering devices. In the past, micron-sized particles with high thermal conductivities were tried to be used within the base fluid to eliminate this drawback. However, it was observed that using micron-sized particles have some other drawbacks such as clogging, sedimentation and high pressure drop. These drawbacks have been overcome by the production of solid particles in nano size with the advancement in technology. Ag, Al, Au, Cu, Fe, diamond, Al_2O_3 , CuO, Fe_3O_4 , TiO_2 and carbon nano tubes have been used as nanoparticles within the base fluid. Nanofluids have a wide variety of applications in the fields of heat transfer (industrial cooling applications, smart fluids, nuclear reactors, extraction of geothermal power and other energy sources), automotive (nanofluid coolant, nanofluid in fuel, brake nanofluids), electronic (cooling of microchips, microscale fluidic applications), biomedical (nanodrug delivery, cryopreservation, nanocryosurgery, ...) (Wong and Leon, 2010). Therefore, over the last decades, nanofluids have been the subject of many studies. Wang et al. (1999) measured the effective thermal conductivity of nanofluids by steady state parallel plate method. They used Al_2O_3 and CuO as nanoparticles and water, vacuum pump fluid, engine oil and ethylene glycol as the base fluid. Their results show that adding 8% Al_2O_3 increases the thermal conductivity of ethylene glycol 40%. They also observed that the measured thermal conductivity of nanofluids is much higher than that of the predicted value by existing models. Xuan and Li (2000) performed a study on the thermal conductivity of nanofluids and developed Nusselt number correlations. They used hot wire method to measure the thermal conductivity of water-based Cu nanofluids. They found that increasing the volume fraction of Cu nanoparticles from 2.5% to 7.5% increases the ratio of the thermal conductivity of nanofluid to that of the base liquid from 1.24 to 1.78. Choi et al. (2001) added nanotubes to oil and found that the thermal conductivity of nanofluid with 1.0

vol. % nanotubes is 160 times greater than that of the oil. They also found that the measured thermal conductivities are significantly higher than the predictions of conventional models. Their study also shows that the measured thermal conductivity shows a non-linear increase with nanotube volume fraction. Xuan and Li (2003) performed an experimental study on the convective heat transfer of water-based Cu nanofluids in a tube. They suggested a Nusselt correlation including the effects of microconvection and microdiffusion of nanoparticles. They also found that the friction factor of water-based Cu nanofluids and water are almost the same. Kang et al. (2006) made an experimental study to measure the thermal conductivity of nanofluids and observed that adding 1% ultra-dispersed diamond increases the effective thermal conductivity of ethylene glycol more than 70%. In another study, Murshed et al. (2008) found that increase in the thermal conductivity of ethylene glycol-based nanofluids is 18% for 5% volumetric loading of TiO_2 particles and 45% for 5% volumetric loading of Al particles. They also found that increase of thermal conductivity of nanofluids with temperature is linear. Li and Peterson (2006) conducted an experimental study to investigate the effects of temperature and volume fraction on the thermal conductivity of nanofluids. Their results show that adding 6% CuO and 10% Al_2O_3 enhances the thermal conductivity of water 1.52 and 1.3 times, respectively. Jang and Choi (2004) suggested a theoretical model accounting the effect of Brownian motion of nanoparticles on the thermal behavior of nanofluids. Murshed et al. (2009) developed a new model combining the static and dynamic effects of thermal conductivity of nanofluids. Cianfrini et al. (2011) performed a theoretical study on natural convection heat transfer of nanofluids in annular spaces between horizontal concentric cylinders. They observed that heat transfer can be enhanced considerably with an optimum particle addition, which depends on temperature and nanoparticle size. Oztop and Abu-Nada (2008) investigated natural convection heat transfer and fluid flow in a partially heated enclosure filled with nanofluids. They observed that heat transfer increases with an increase in Rayleigh number and heater size. Kahveci (2010) investigated buoyancy driven heat transfer of nanofluids in a tilted enclosure for different values of Rayleigh number, solid volume fraction, ratio of nanolayer thickness to the original particle radius and inclination angle. The results show that maximum heat transfer takes place at 45 deg. for $\text{Ra}=10^4$ and at 30 deg. for $\text{Ra}=10^5, 10^6$. Pak and Choi (1998) conducted an experimental investigation on the turbulent flow of nanofluids with metallic oxide particles in a circular pipe. They found that the convective heat transfer coefficient of nanofluid with 3% solid volume fraction is 12% smaller than that of water for a given average fluid velocity. Lai and Yang (2011) found that heat transfer shows an increase with the increase of particle volume fraction and Rayleigh number for the water-based Al_2O_3 nanofluid in a square enclosure. They also found that heat transfer rate of nanofluid is lower than that of water at a fixed temperature difference because of relatively high dynamic viscosity of nanofluids. Yu et al. (2011) made a numerical

study on the laminar natural convection of water-based CuO nanofluids in a horizontal triangular enclosure. Their results show that, when the Grashof number is greater than a critical value, a pitchfork bifurcation is observed. Rahman et al. (2011) numerically investigated the mixed convection of nanofluids in an inclined lid-driven triangular enclosure. They observed that the effect of the solid volume fraction on the flow field is greater than its effect on the thermal field. Susantez et al. (2012) investigated buoyancy driven heat transfer of nanofluids in a square enclosure with a heat conducting solid circular body at the center for various values of the ratio of the thermal conductivity of the solid cylinder to that of the base fluid. The results show that the effect of the ratio of thermal conductivity of the solid cylinder to that of the base fluid on heat transfer rate is negligible. Cihan et al. (2012) investigated convective heat transfer in an inclined square enclosure with a solid cylinder at the center and found that maximum heat transfer takes place at 45° for Ra=10⁴ and 30° for Ra=10⁵ and Ra=10⁶.

From the literature given above, it can be seen that there is a limited number of studies on heat transfer and fluid flow of nanofluids in an enclosure with a conducting solid body and the effects of the several parameters such as aspect ratio of the enclosure, cylinder diameter and location on flow and heat transfer have not been studied yet. Accordingly, heat transfer enhancement of water-based CuO nanofluids in a rectangular enclosure with a solid conducting body was investigated numerically in this study for different values of aspect ratio, diameter and location of the solid cylinder, solid volume fraction, and Rayleigh number.

ANALYSIS

The schematic view of the enclosure geometry used in the study is seen in Fig. 1. While sidewalls of the enclosure are at constant temperature, upper and bottom walls are in adiabatic conditions.

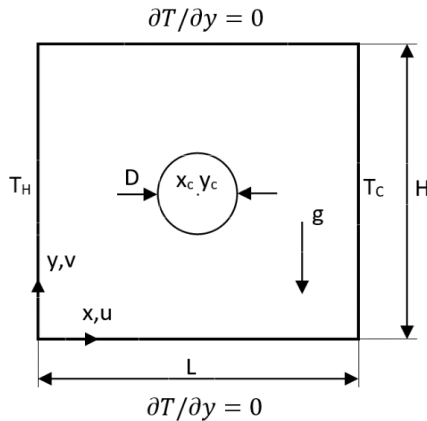


Figure 1. Geometry and coordinate system

Under the assumption of two dimensional, Newtonian, steady and incompressible flow with constant thermophysical properties, the governing equations take the following form:

Continuity equation:

$$u \frac{\partial u}{\partial x} + v \frac{\partial v}{\partial y} = 0 \quad (1)$$

Momentum equations:

$$u \frac{\partial u}{\partial x} + v \frac{\partial u}{\partial y} = -\frac{1}{\rho_{eff}} \frac{\partial P}{\partial x} + \frac{\mu_{eff}}{\rho_{eff}} \left[\frac{\partial^2 u}{\partial x^2} + \frac{\partial^2 u}{\partial y^2} \right] \quad (2)$$

$$u \frac{\partial v}{\partial x} + v \frac{\partial v}{\partial y} = -\frac{1}{\rho_{eff}} \frac{\partial P}{\partial y} + \frac{\mu_{eff}}{\rho_{eff}} \left[\frac{\partial^2 v}{\partial x^2} + \frac{\partial^2 v}{\partial y^2} \right] + g\beta_{T,eff}(T - T_c) \quad (3)$$

Energy equation:

$$u \frac{\partial T}{\partial x} + v \frac{\partial T}{\partial y} = \frac{k_{eff}}{(\rho c_p)_{eff}} \left[\frac{\partial^2 T}{\partial x^2} + \frac{\partial^2 T}{\partial y^2} \right] \quad (4)$$

Energy equation for the solid cylinder:

$$\frac{\partial^2 T}{\partial x^2} + \frac{\partial^2 T}{\partial y^2} = 0 \quad (5)$$

The governing equations are nondimensionalized by the following nondimensional variables:

$$x^* = \frac{x}{L}, y^* = \frac{y}{L}, u^* = \frac{u}{\frac{L}{\alpha_f}}, v^* = \frac{v}{\frac{L}{\alpha_f}}, \quad (6)$$

$$P^* = \frac{L^2}{\rho_f \alpha_f^2} P, T^* = \frac{T - T_c}{T_H - T_c}$$

where u^* and v^* dimensionless velocity components, P^* is dimensionless pressure, T^* is dimensionless temperature, α_f and ρ_f are thermal diffusivity and density of the base fluid, respectively.

The corresponding nondimensional form of the governing equations are as follows:

$$\frac{\partial u^*}{\partial x^*} + \frac{\partial v^*}{\partial y^*} = 0 \quad (7)$$

$$\frac{\rho_{eff}}{\rho_f} u^* \frac{\partial u^*}{\partial x^*} + \frac{\rho_{eff}}{\rho_f} v^* \frac{\partial u^*}{\partial y^*} = -\frac{\partial P^*}{\partial x^*} + \frac{\rho_{eff} \nu_{eff}}{\rho_f \nu_f} Pr \left[\frac{\partial^2 u^*}{\partial x^{*2}} + \frac{\partial^2 u^*}{\partial y^{*2}} \right] \quad (8)$$

$$\frac{\rho_{eff}}{\rho_f} u^* \frac{\partial v^*}{\partial x^*} + \frac{\rho_{eff}}{\rho_f} v^* \frac{\partial v^*}{\partial y^*} = -\frac{\partial P^*}{\partial y^*} + \frac{\rho_{eff} \nu_{eff}}{\rho_f \nu_f} Pr \left[\frac{\partial^2 v^*}{\partial x^{*2}} + \frac{\partial^2 v^*}{\partial y^{*2}} \right] \quad (9)$$

$$+ Ra Pr \frac{(\rho \beta_T)_{eff}}{(\rho \beta_T)_f} T^* \quad (10)$$

$$u^* \frac{\partial T^*}{\partial x^*} + v^* \frac{\partial T^*}{\partial y^*} = \frac{\alpha_{eff}}{\alpha_f} \left[\frac{\partial^2 T^*}{\partial x^{*2}} + \frac{\partial^2 T^*}{\partial y^{*2}} \right] \quad (11)$$

$$\frac{\partial^2 T^*}{\partial x^{*2}} + \frac{\partial^2 T^*}{\partial y^{*2}} = 0 \quad (11)$$

where aspect ratio, Prandtl and Rayleigh numbers are defined as:

$$ar = \frac{H}{L}, Pr = \frac{\nu_f}{\alpha_f}, Ra = \frac{g \beta_{T,f} L^3 \Delta T}{\nu_f \alpha_f} \quad (12)$$

where g is gravitational acceleration, ΔT is the temperature difference between the isothermal walls of the enclosure, $\beta_{T,f}$ and ν_f are thermal expansion coefficient and kinematic viscosity of the base fluid, respectively.

The governing equations are subjected to the following boundary conditions:

$$T^*|_{0,y^*} = 1, T^*|_{1,y^*} = 0, \quad \frac{dT^*}{dy}\Big|_{x^*,0} = 0, \quad \frac{dT^*}{dy}\Big|_{x^*,ar} = 0 \quad (13)$$

$$u^*|_{0,y^*} = 0, \quad u^*|_{1,y^*} = 0, \quad u^*|_{x^*,0} = 0, \quad u^*|_{x^*,ar} = 0, \quad u^*|_S = 0 \quad (14)$$

$$v^*|_{0,y^*} = 0, \quad v^*|_{1,y^*} = 0, \quad v^*|_{x^*,0} = 0, \quad v^*|_{x^*,ar} = 0, \quad v^*|_S = 0 \quad (15)$$

The thermal boundary conditions for the surface of the solid cylinder are based on the continuity of heat flux and thermal equilibrium:

$$\vec{n} \cdot (\vec{q}_1 - \vec{q}_2) = 0 \quad (16)$$

$$T_1 = T_2 \quad (17)$$

where \vec{n} is unit normal vector. The subscripts 1 and 2 represent nanofluid and solid cylinder, respectively. From the heat flux continuity equation an extra parameter k^* , which is the ratio of the thermal conductivity of the solid cylinder to that of the base fluid, emerges. In this study, it was assumed that the thermal conductivity of the solid cylinder is equal to that of the base fluid.

Thermal conductivity of the nanofluid is one of the most important parameters related to the heat transfer performance of nanofluids. As there is not a theoretical model for the thermal conductivity of nanofluids, models for solid-liquid mixtures are generally used for this purpose. One of these types of model is Maxwell model (Maxwell, 1873) defined as:

$$\frac{k_{eff}}{k_f} = \frac{k_s + 2k_f + 2(k_s - k_f)\phi}{k_s + 2k_f - (k_s - k_f)\phi} \quad (18)$$

where k_s and k_f are the thermal conductivity of solid particles and base fluid, respectively, and ϕ is the nanoparticle volume fraction.

Another model proposed by Hamilton and Crosser (1962) for two component mixtures with nonspherical particles takes into account the effect of the shape of particles.

$$\frac{k_{eff}}{k_f} = \frac{k_s + (n-1)k_f + (n-1)(k_s - k_f)\phi}{k_s + (n-1)k_f - (k_s - k_f)\phi} \quad (19)$$

The shape factor n is defined as a function of sphericity Ψ as $n = 3/\Psi$.

Yu and Choi (2003) proposed a thermal conductivity model based on liquid layering around solid particles. With the assumption of $k_{layer} = k_s$ this model for spherical particles takes the following form:

$$\frac{k_{eff}}{k_f} = \frac{k_s + 2k_f + 2(k_s - k_f)(1 + \beta)^3\phi}{k_s + 2k_f - (k_s - k_f)(1 + \beta)^3\phi} \quad (20)$$

where, β is the ratio of the liquid layering thickness to the original particle radius. This model was used in the present study for the effective thermal conductivity of nanofluids by assuming that $\beta = 0.1$, which is a value that produces good agreements with experimental thermal conductivity data.

To estimate the effective viscosity of nanofluid, the Brinkman model (Brinkman, 1952) was used in this study.

$$\mu_{eff} = \mu_f / (1 - \phi)^{2.5} \quad (21)$$

The other effective properties of nanofluids can be defined as follows:

$$(\rho c_p)_{eff} = (1 - \phi)(\rho c_p)_f + \phi(\rho c_p)_s \quad (22)$$

$$(\rho \beta_T)_{eff} = (1 - \phi)(\rho \beta_T)_f + \phi(\rho \beta_T)_s \quad (23)$$

$$\rho_{eff} = (1 - \phi)\rho_f + \phi\rho_s \quad (24)$$

The local and average Nusselt number along the hot isothermal wall of the enclosure can be defined as follows:

$$Nu = -\frac{k_{eff}}{k_f} \frac{\partial T^*}{\partial x^*}\Big|_{x^*=0} \quad (25)$$

$$Nu_a = \frac{1}{ar} \int_0^{ar} Nu dy^* \quad (26)$$

RESULTS AND DISCUSSION

Numerical simulations were performed by Comsol Multiphysics finite element modeling and simulation software. The parallel direct sparse solver (Pardiso), which is a high performance and memory efficient solver, was used for the solutions.

The thermophysical properties of the base fluid and nanoparticle used in the study were given in Table 1. The Prandtl number of the base fluid is 6.2.

Table 1. The thermophysical properties of the base fluid and nanoparticle

Property	Water	CuO
$\rho(kg/m^3)$	997.1	6500
$c_p(J/kg K)$	4179	536
$k(W/m K)$	0.613	20
$\alpha \cdot 10^7(m^2/s)$	1.47	57.4
$\beta_T \cdot 10^6(1/K)$	210	51
Pr	6.2	-

A mesh dependency test was also carried out in this study (see Table 2 and 3). The average Nusselt number on the hot wall was obtained for each mesh case. It is seen from Table 2 that the case 5 is appropriate to have mesh independent results. Therefore, it was used in the simulations in the study.

Table 2. The number of mesh elements used in mesh dependency study

Case	Number of elements	Edge elements	Number of degrees of freedom
1	1114	116	2231
2	2224	196	4611
3	6194	350	12724
4	17362	440	34859
5	27908	594	55660

Table 3. Average Nusselt numbers for $ar = 0.5$, $D/L = 0.125$, $x_c^* = 0.5$, $y_c^* = 0.25$, $\phi = 0$

Case	Ra=10 ⁴	Ra=10 ⁶
1	1.2277	8.5768
2	1.2354	9.0693
3	1.2386	9.1663
4	1.2406	9.1979
5	1.2409	9.2062

Numerical results were validated by comparing the results of this study with the results of Khanafer et al. (2003) and Kahveci (2010) (see Tables 4 and 5). An acceptable agreement is seen between the results. The main reason of

relatively higher difference between the results of this study and Khanafer et al. (2003) is different thermal effective conductivity models used for the nanofluid.

Table 4. Validation of the results for water-based Cu nanofluid

	Gr/Ø	0	0.04	0.08	0.12	0.16	0.2
Present	10 ³	1.934	2.053	2.167	2.282	2.408	2.560
Khanafer et al. (2003)	10 ³	1.948	2.100	2.251	2.418	2.584	2.766
Present	10 ⁴	4.078	4.367	4.645	4.916	5.182	5.446
Khanafer et al. (2003)	10 ⁴	4.089	4.375	4.705	5.035	5.365	5.710

Table 5. Validation of the results for water-based CuO nanofluid

	Ra/Ø	0.05	0.10	0.15	0.20
Present	10 ⁴	2.466	2.650	2.828	3.005
Kahveci (2010)	10 ⁴	2.466	2.651	2.829	3.005
Present	10 ⁵	5.163	5.597	6.025	6.450
Kahveci (2010)	10 ⁵	5.165	5.599	6.027	6.452
Present	10 ⁶	10.143	11.074	12.008	12.953
Kahveci (2010)	10 ⁶	10.160	11.089	12.022	12.966

Temperature distribution and velocity field in the enclosure are seen in Figs. 2, 3 and 4 for various values of the parameters considered in this study. As it can be observed from the figures that a clockwise rotating circulation is formed in the flow field. Circulation intensity increases considerably with an increase in the Rayleigh number as a result of strengthening convection. As it can also be seen from the temperature distribution that flow regime evolves to the boundary layer flow regime with an increase in the Rayleigh number. As the Rayleigh number increases, the thickness of the thermal boundary layer decreases. As it can be observed from the figures that circulation intensity generally shows a small decrease with an increase in the solid volume fraction for low values of the Rayleigh number as a result of increase in the viscosity. On the other hand, circulation intensity shows an increase with an increase in the solid volume fraction for high values of the Rayleigh number. This can be attributed to the relatively weak viscous forces in high Rayleigh numbers. With an increase in solid volume fraction, both thermal conductivity and viscosity of the nanofluid increases. For low values of Rayleigh number,

the effect of viscosity increase on flow is in important levels as a result of relatively significant viscous forces. The effect of viscosity on flow decreases with an increase in the Rayleigh number as a result of relatively lower viscous forces. Therefore, circulation weakens for low Rayleigh number and strengthens for high Rayleigh numbers with an increase in the solid volume fraction. As it can be seen from Fig. 3 that circulation intensity shows a considerable decrease with an increase in the diameter of the cylinder especially for low values of Rayleigh number. As it can also be seen from Figure 3 that maximum velocity shows a decrease or increase with a change of cylinder location depending on the obstruction level of the cylinder on flow and depending on the decrease in flow cross section. It can also be concluded from Figs. 2-4 that circulation intensity shows an increase with an increase in the aspect ratio as a result of higher heat transfer surface area.

The variation of the average Nusselt number with the solid volume fraction is seen in Figs. 5-7 for various values of the parameters considered in this study. As it can be seen from these figures that the average Nusselt number shows a linear increase with the solid volume fraction. It can also be observed that the average Nusselt number shows a significant increase with the Rayleigh number. The average heat transfer rate shows a decrease with an increase in the diameter of the solid cylinder inside the enclosure. As it can be seen from Figs. 5-7 that the heat transfer rate shows an increase with an increase of aspect ratio for low values of Rayleigh number. Highest value of heat transfer rate is for square enclosure case for high values of Rayleigh number.

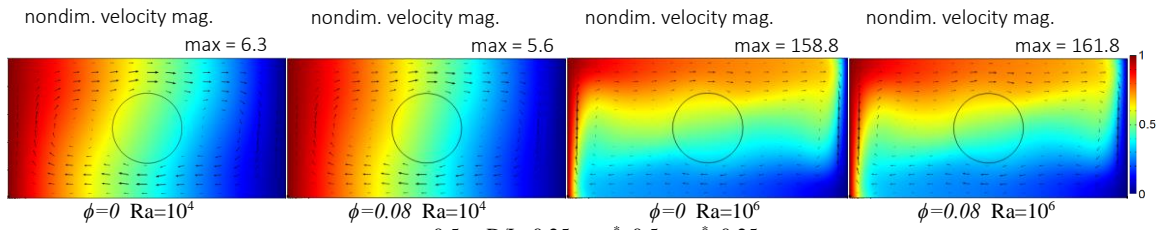


Figure 2. Temperature distribution and velocity field of water-based CuO nanofuid for $ar = 0.5$

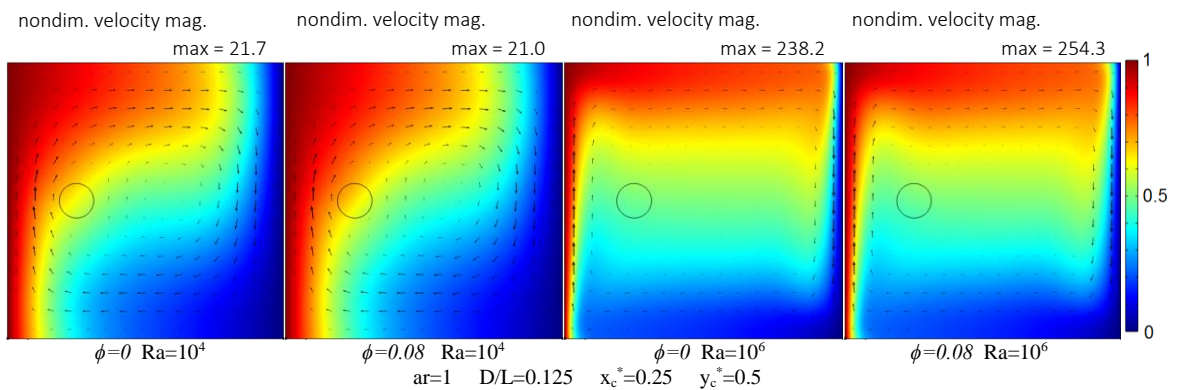
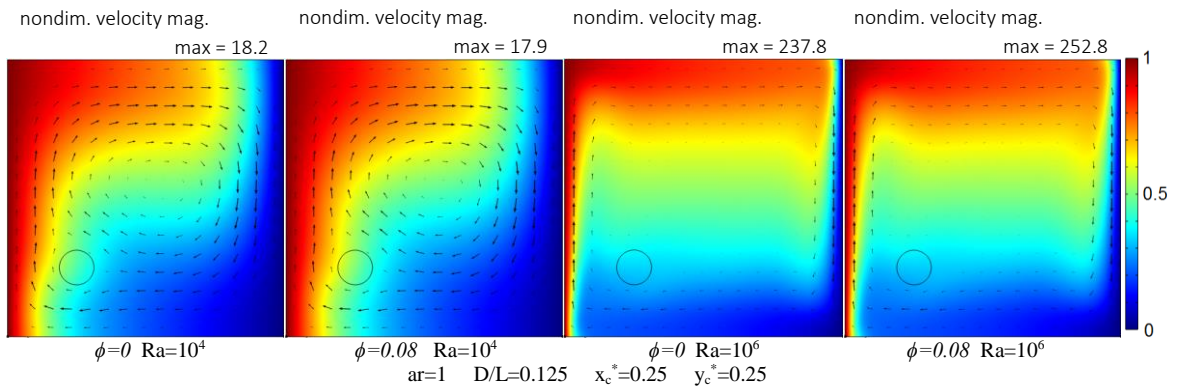
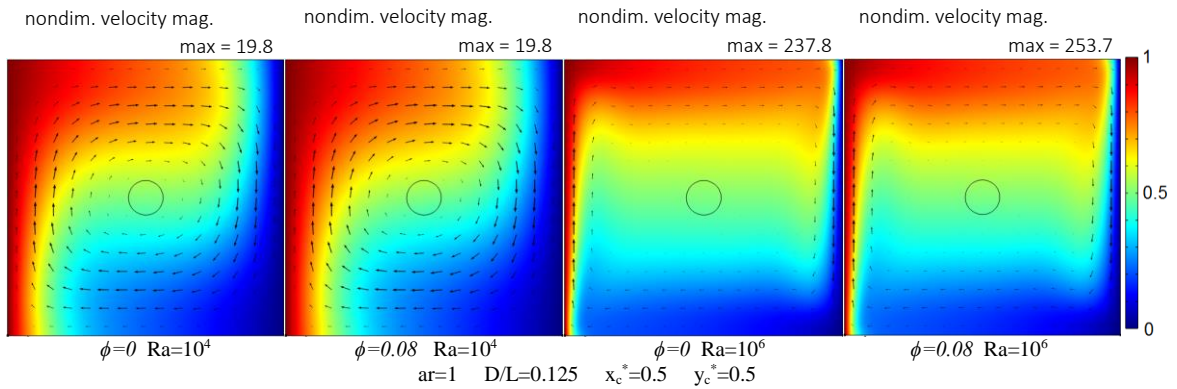


Figure 3a. Temperature distribution and velocity field of water-based CuO nanofuid for $ar = 1$

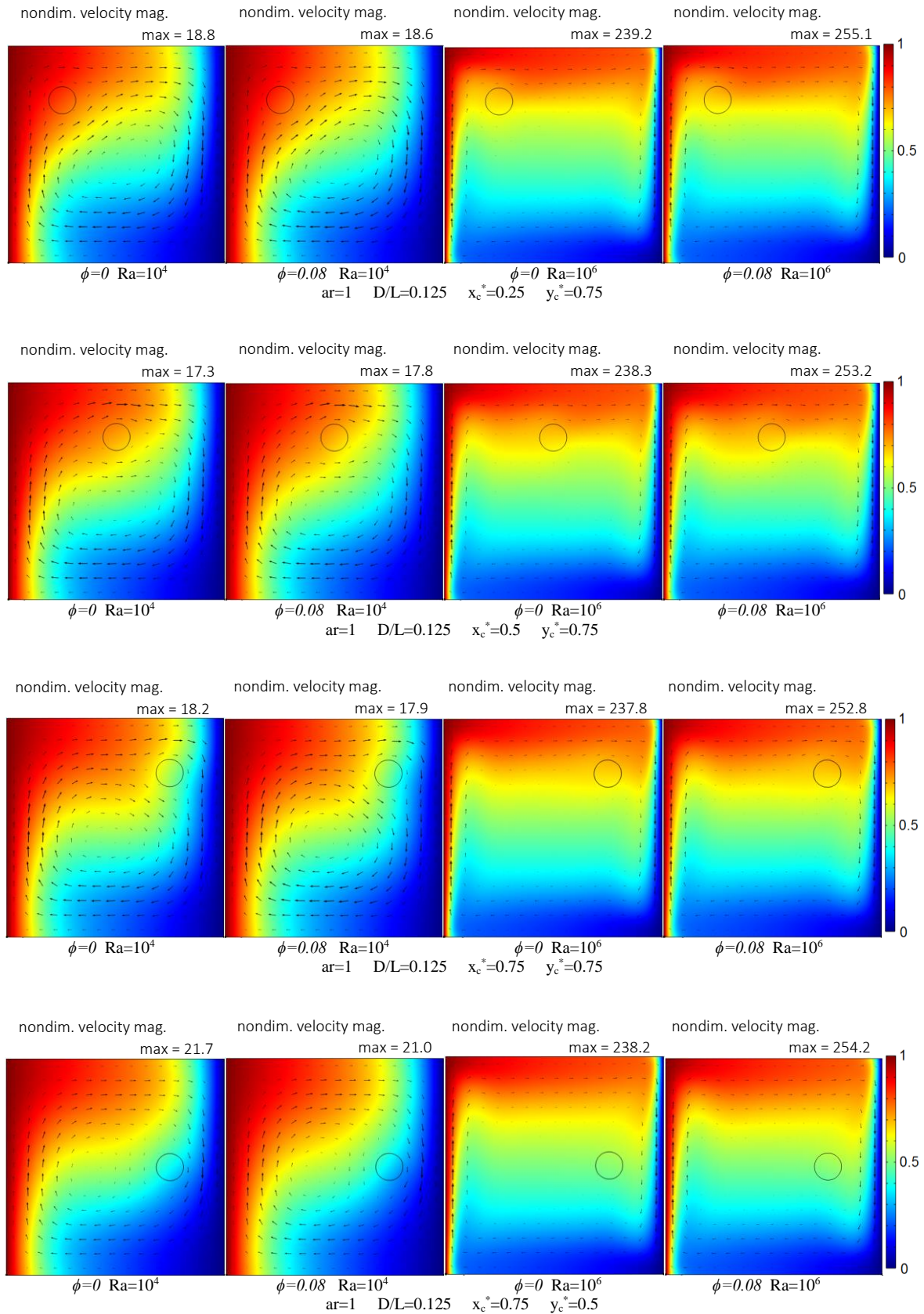


Figure 3b. Temperature distribution and velocity field of water-based CuO nanofuid for $ar = 1$

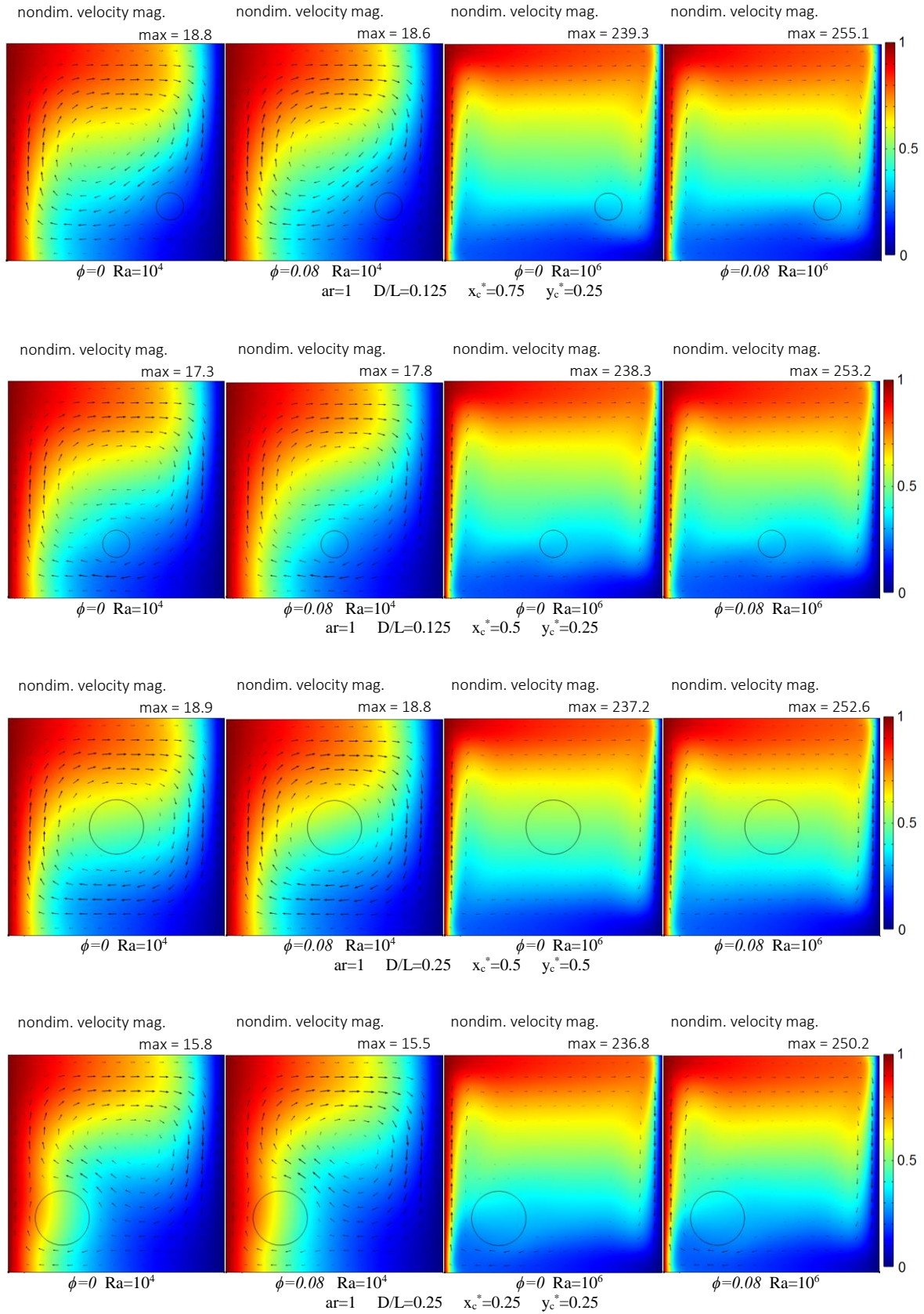


Figure 3c. Temperature distribution and velocity field of water-based CuO nanofluid for $ar=1$

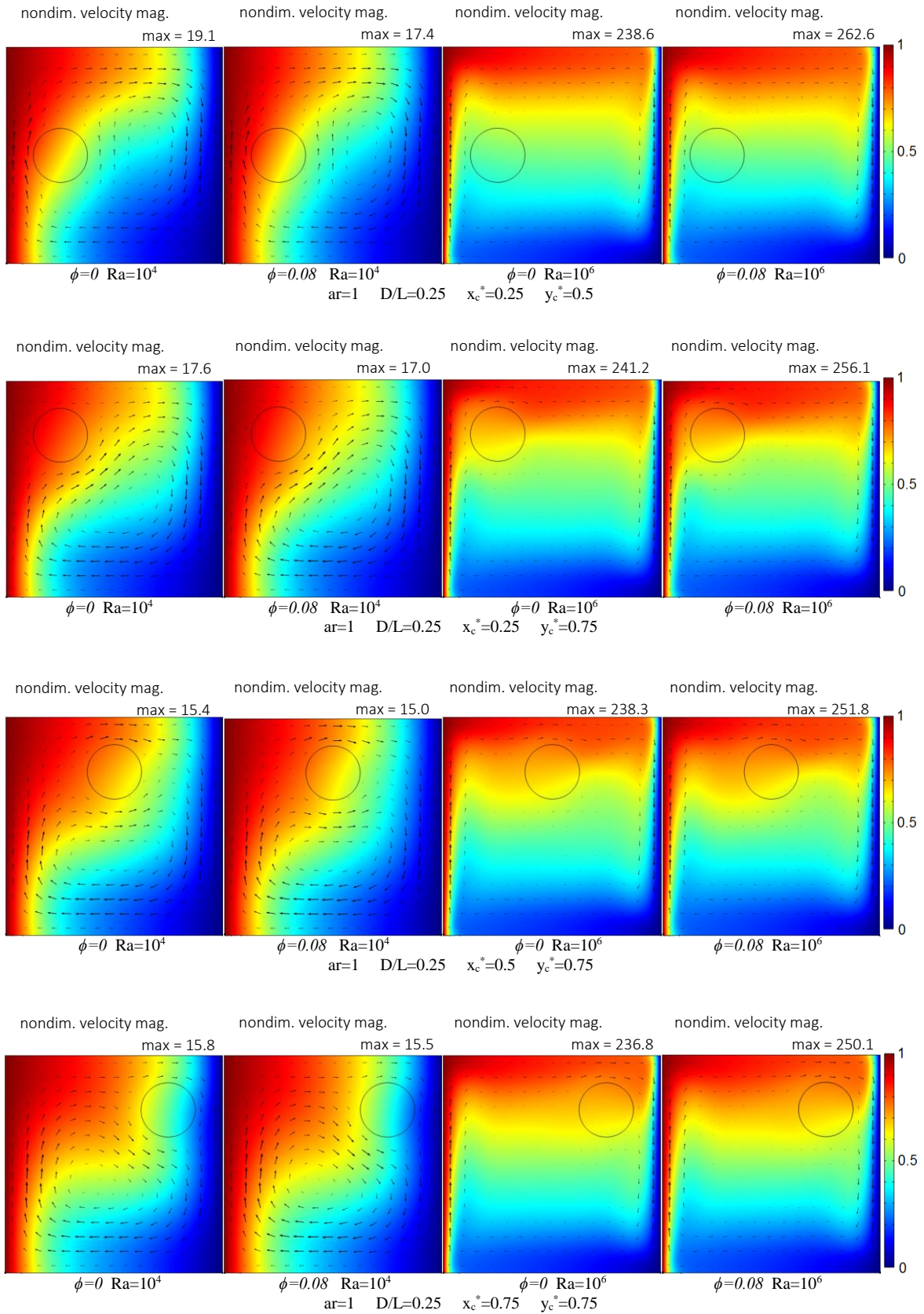


Figure 3d. Temperature distribution and velocity field of water-based CuO nanofuid for $ar=1$

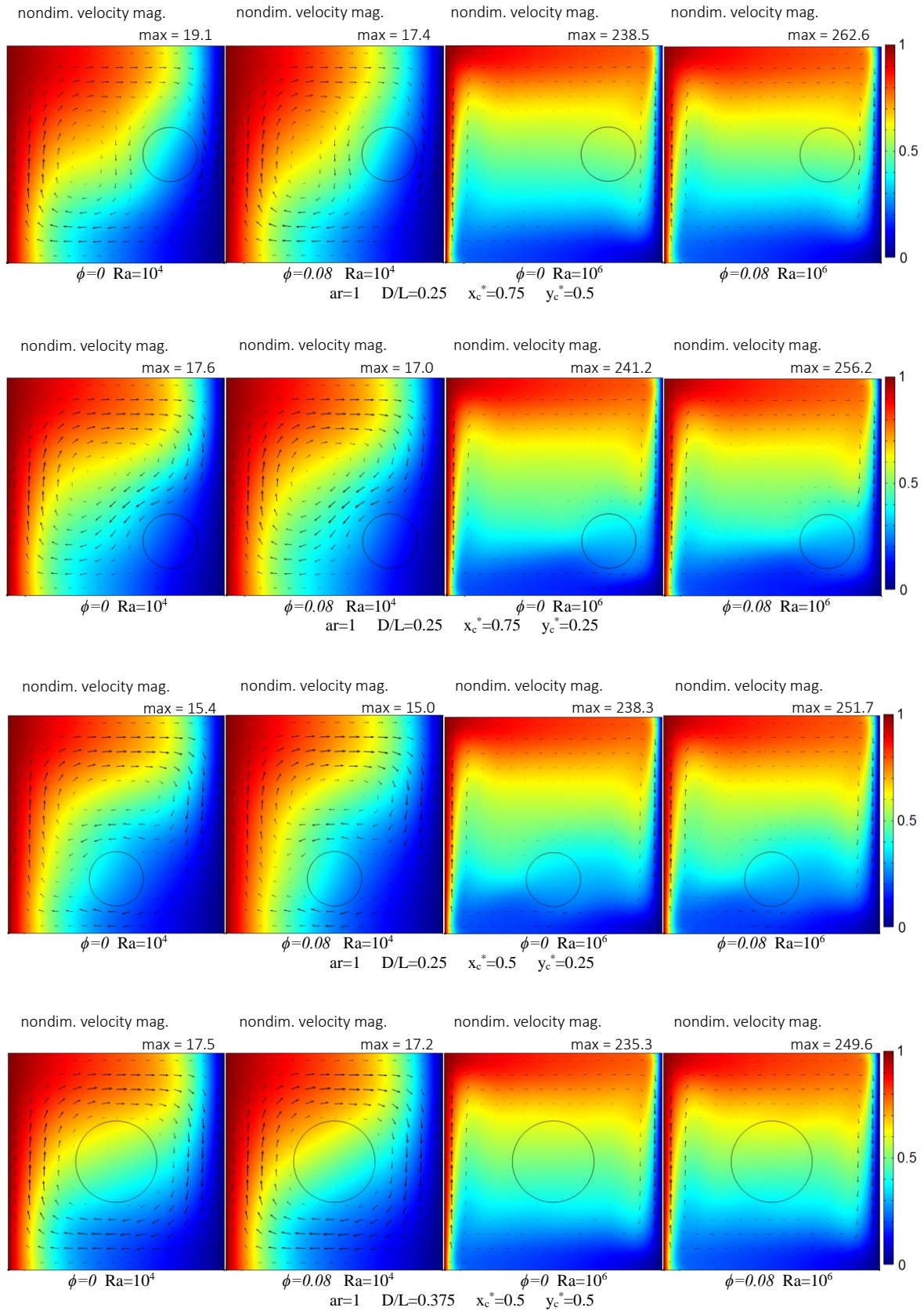


Figure 3e. Temperature distribution and velocity field of water-based CuO nanofluid for $ar=1$

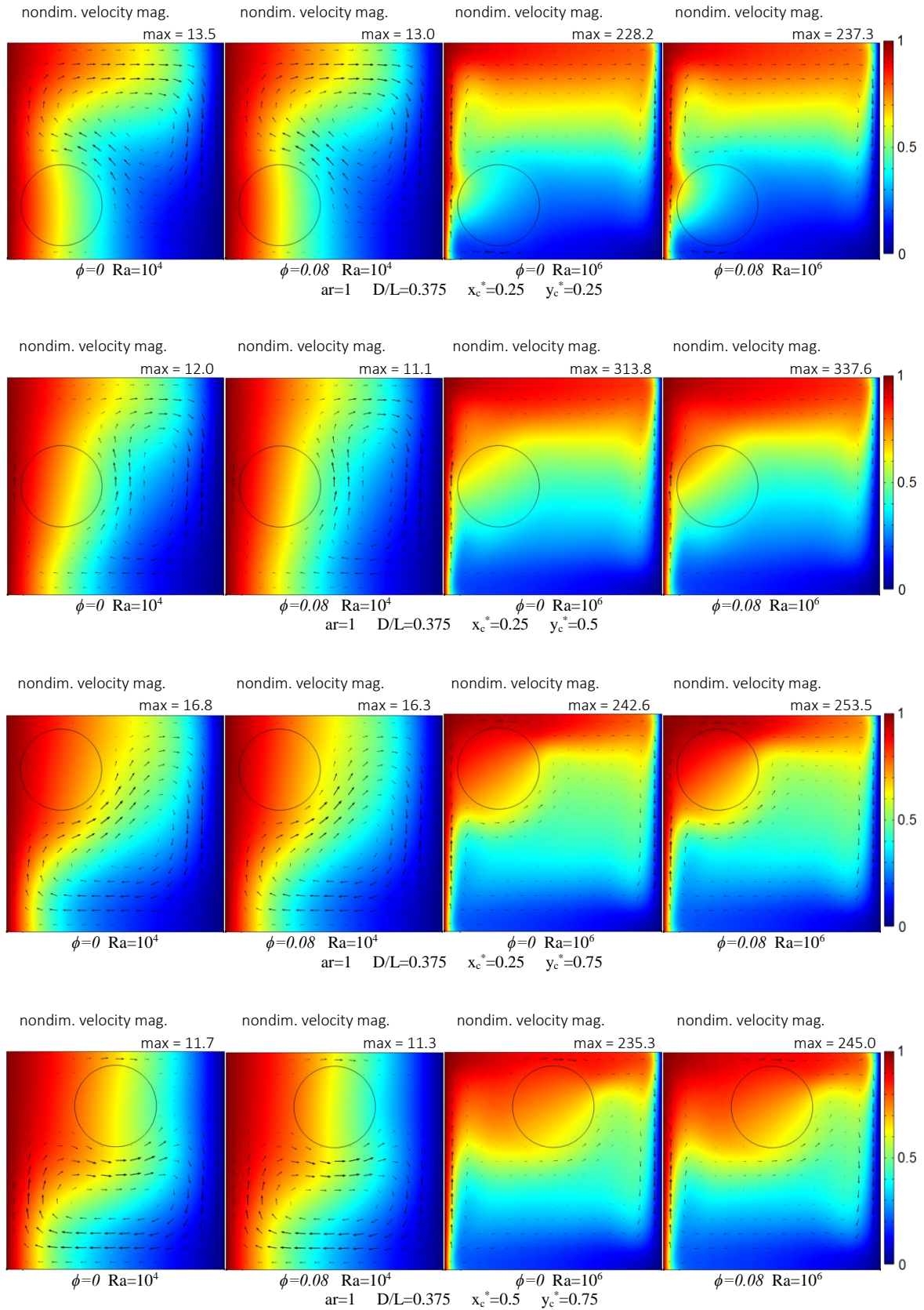


Figure 3f. Temperature distribution and velocity field of water-based CuO nanofuid for ar =1

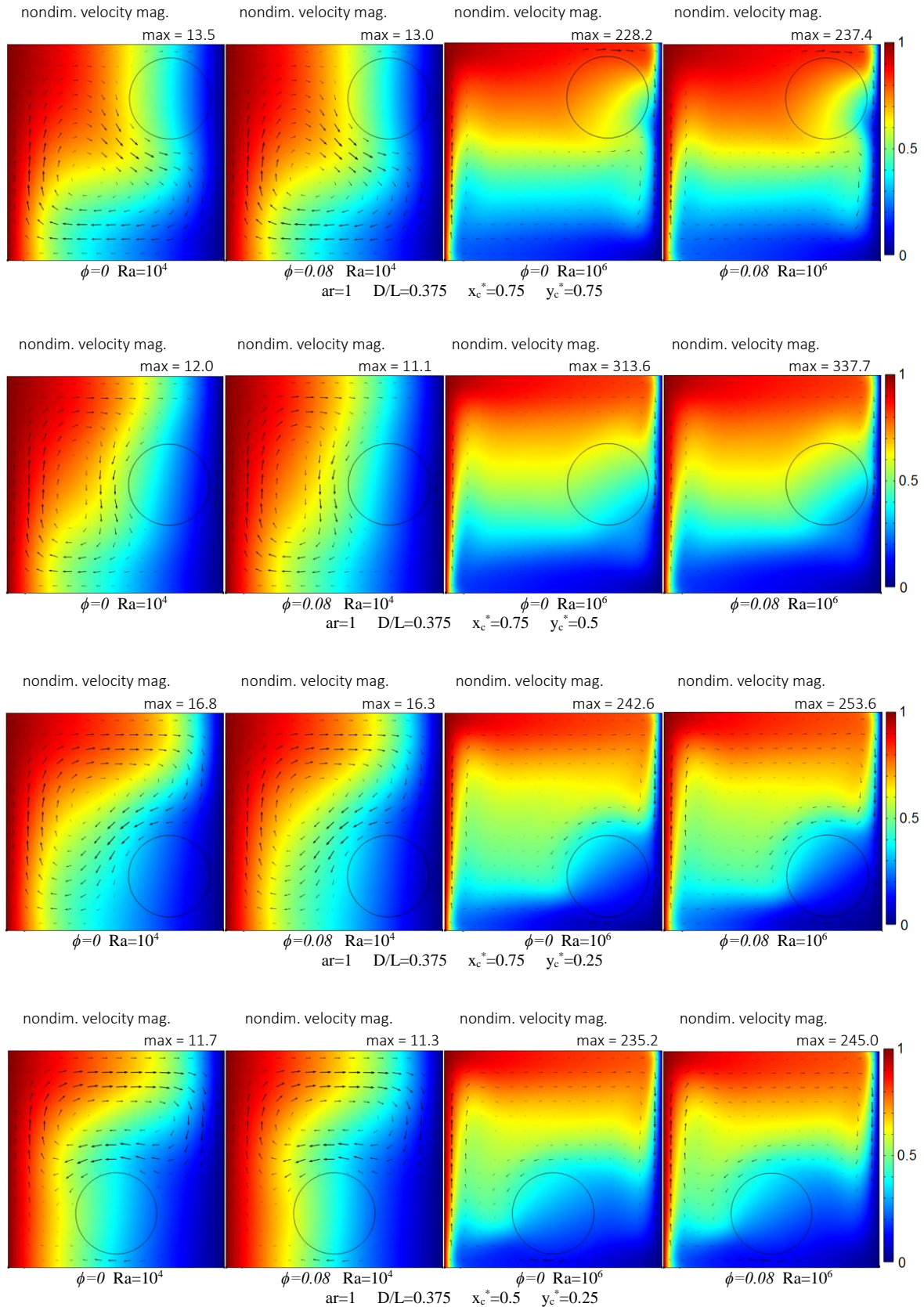


Figure 3g. Temperature distribution and velocity field of water-based CuO nanofluid for $ar=1$

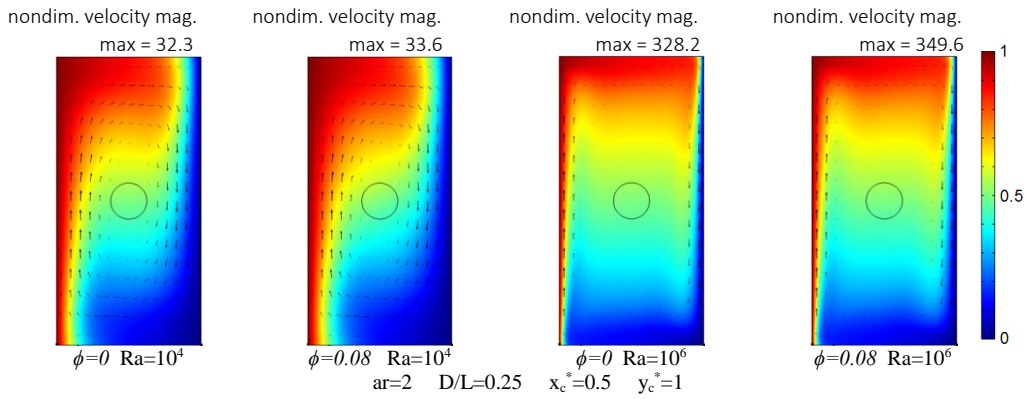


Figure 4. Temperature distribution and velocity field of water-based CuO nanofluid for $ar = 2$

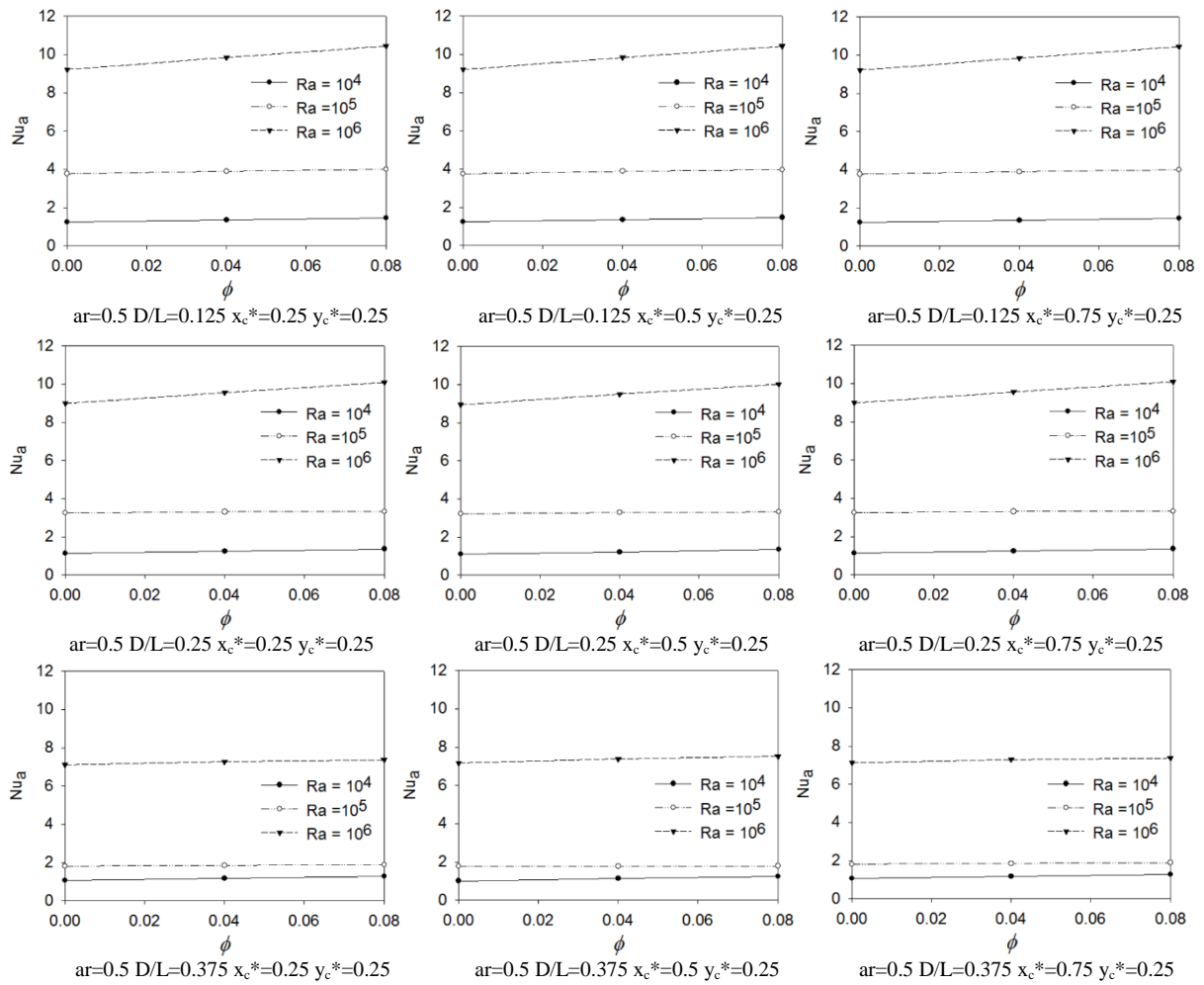


Figure 5. Average Nusselt number for $ar = 0.5$

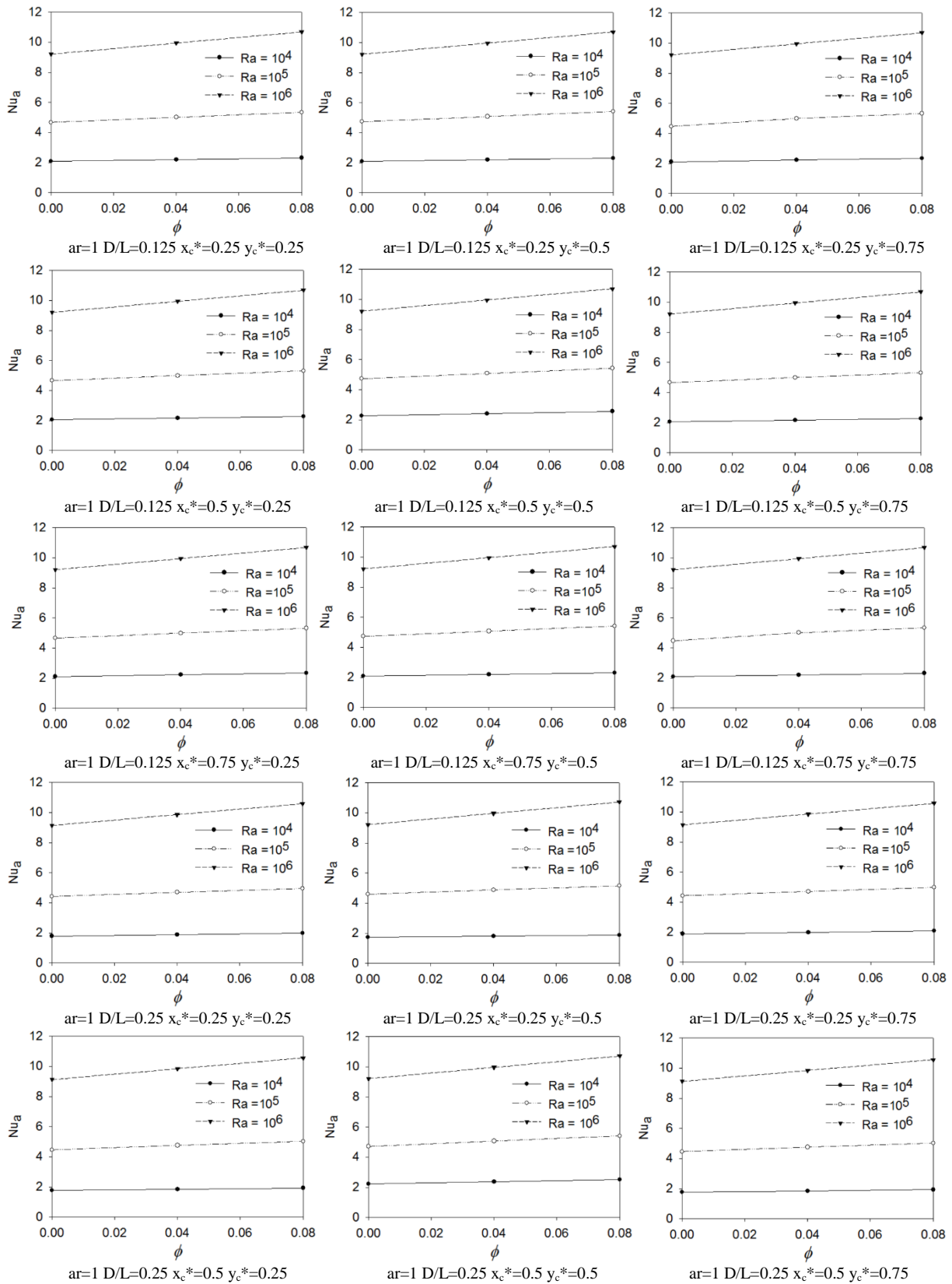


Figure 6a. Average Nusselt number for $ar = 1$

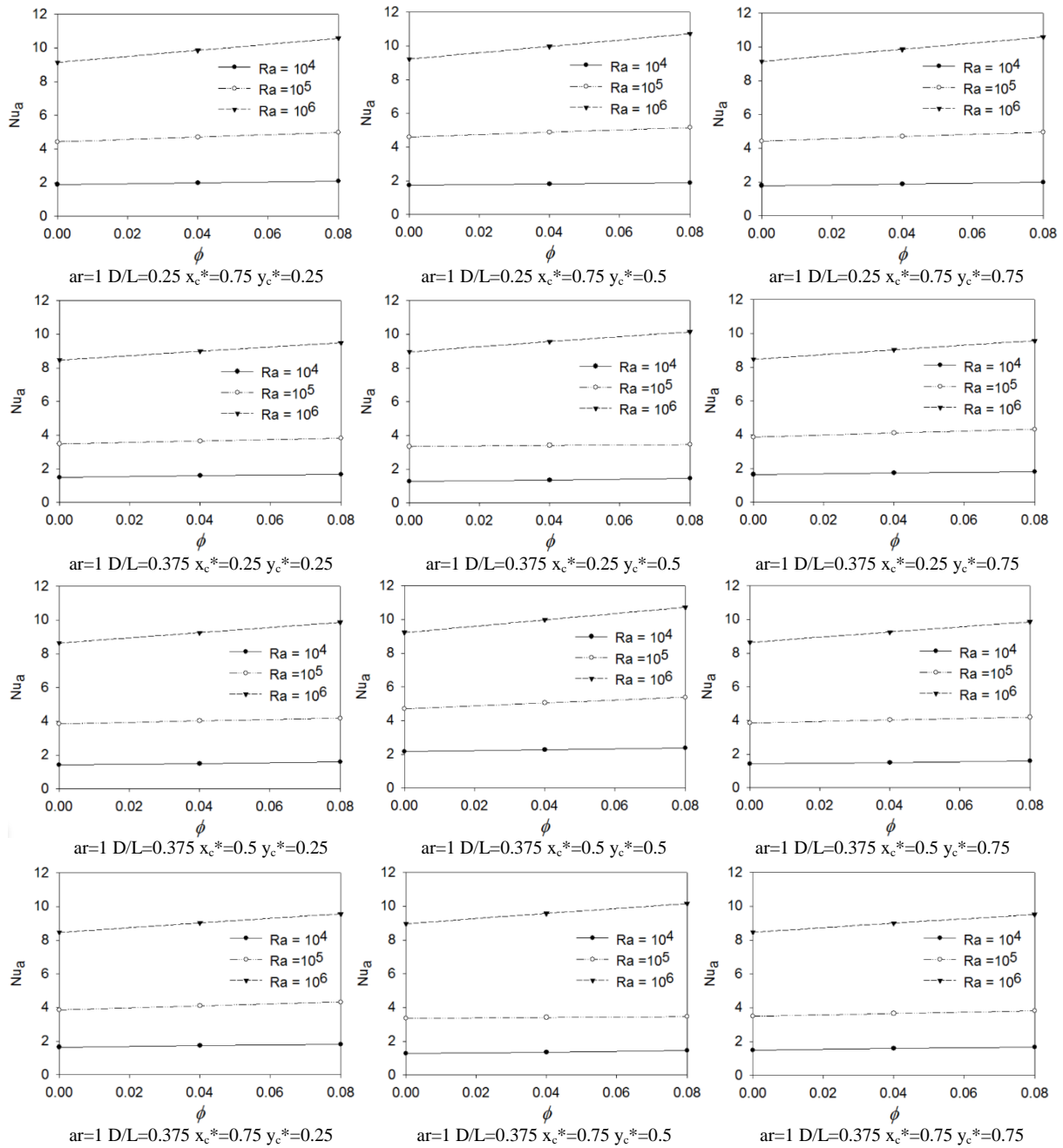


Figure 6b. Average Nusselt number for $ar = 1$

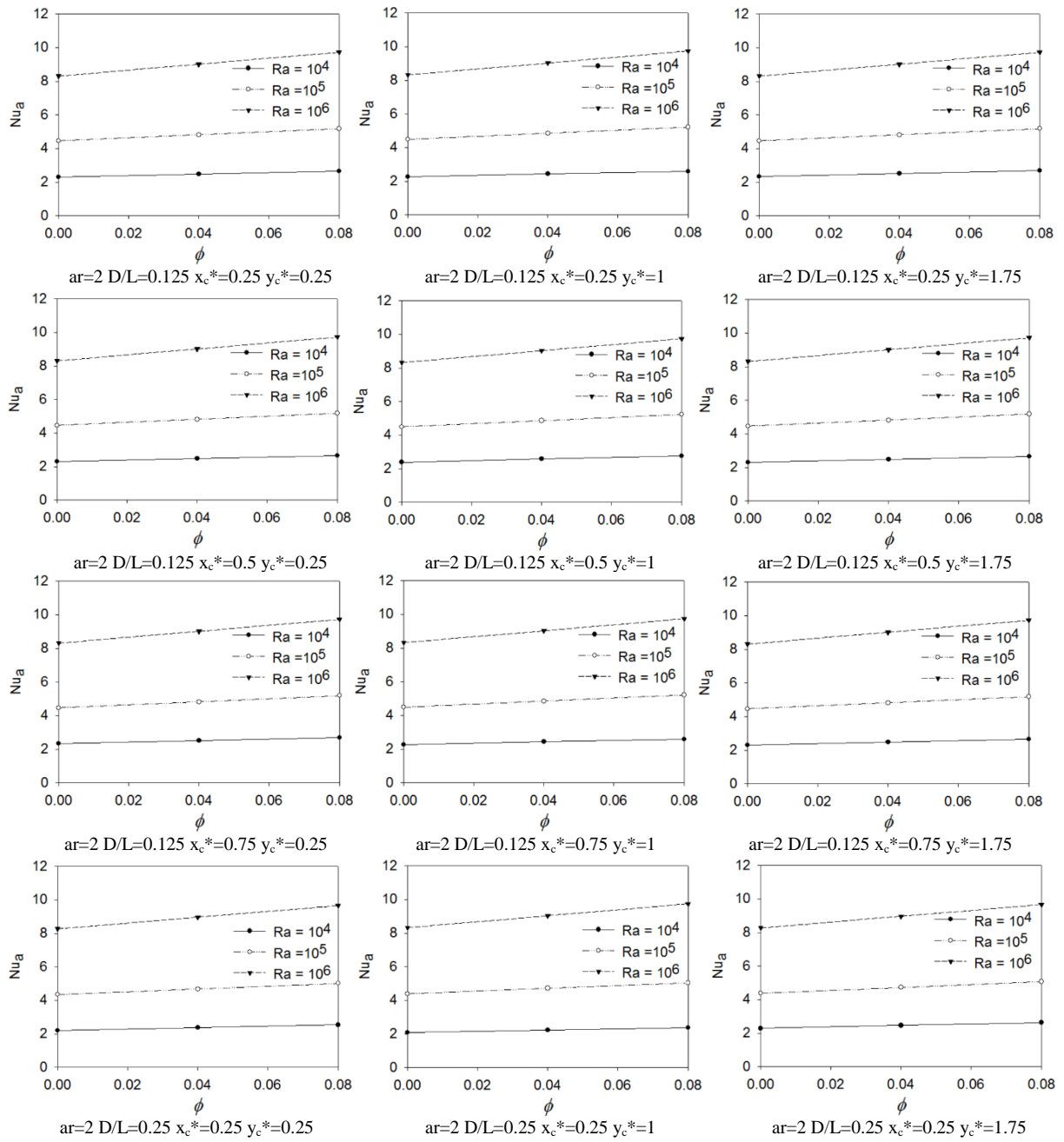


Figure 7a. Average Nusselt number for $ar = 2$

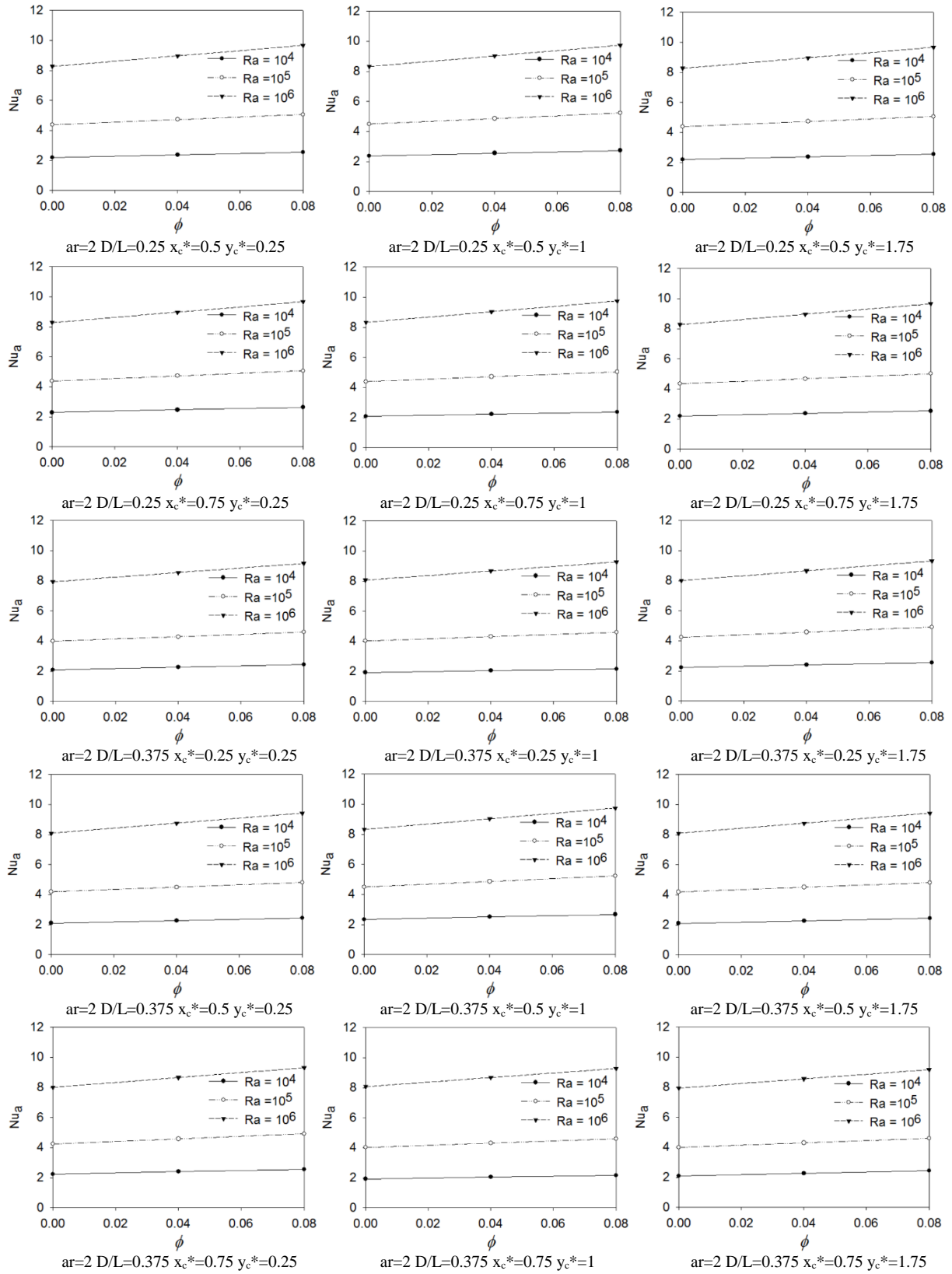


Figure 7b. Average Nusselt number for $ar = 2$

CONCLUSION

In this paper, heat transfer enhancement of water-based CuO nanofluids in an enclosure with a solid conducting body was investigated numerically by Comsol Multiphysics finite element modeling and simulation software. Computational results were obtained for various values of aspect ratio of the enclosure, diameter and location of the solid cylinder, Rayleigh number and solid volume fraction. It was observed that adding nanoparticles causes an increase in heat transfer rate. The effect of Rayleigh number on heat transfer rate is more significant than that of the solid volume fraction. With an increase of the diameter of cylinder inside the enclosure, heat transfer rate gets lower values. Heat transfer rate shows an increase with an increase of aspect ratio for low values of Rayleigh number. On the other hand, heat transfer rate gets its highest value for square enclosure case for high values of Rayleigh number.

REFERENCES

- Brinkman H. C., 1952, The Viscosity of Concentrated Suspensions and Solutions, *J. Chem. Phys.*, 20, 571-581.
- Choi S. U. S., Zhang Z. G., Yu W., Lockwood F. E. and Grulke E. A., 2001, Anomalous Thermal Conductivity Enhancement in Nanotube Suspensions, *Appl. Phys. Lett.*, 79(14), 2252-2254.
- Cianfrini M., Corcione M. and Quintino A., 2011, Natural Convection Heat Transfer of Nanofluids in Annular Spaces Between Horizontal Concentric Cylinders, *Appl. Therm. Eng.*, 31(17-18), 4055-4063.
- Cihan A., Kahveci K. and Susantez Ç., 2012, Buoyancy Driven Heat Transfer of Water-Based CuO Nanofluids in a Tilted Enclosure with a Heat Conducting Solid Cylinder on Its Center, *World Congress on Engineering*, London, 1750-1754.
- Hamilton R. L., and Crosser O. K., 1962, Thermal Conductivity of Heterogeneous Two-Component Systems, *Ind. Eng. Chem. Fundam.*, 1(3), 187-191.
- Jang S. P. and Choi S. U. S., 2004, Role of Brownian Motion in the Enhanced Thermal Conductivity of Nanofluids, *Appl. Phys. Lett.*, 84(21), 4316-4318.
- Kahveci K., 2010, Buoyancy Driven Heat Transfer of Nanofluids in a Tilted Enclosure, *J. Heat Transfer*, 132(6), 062501.
- Kang H. U., Kim S. H. and Oh J. M., 2006, Estimation of Thermal Conductivity of Nanofluid Using Experimental Effective Particle Volume, *Exp. Heat Transfer*, 19(3), 181-191.
- Khanafer K., Vafai K. and Lightstone M., 2003, Buoyancy-driven heat transfer enhancement in a two-dimensional enclosure utilizing nanofluids, *Int. J. Heat Mass Tran.*, 46, 3639-3653.
- Lai F. H. and Yang Y. T., 2011, Lattice Boltzmann Simulation of Natural Convection Heat Transfer of Al₂O₃/water Nanofluids in a Square Enclosure, *Int. J. Therm. Sci.*, 50(10), 1930-1941.
- Li C. H. and Peterson G. P., 2006, Experimental Investigation of Temperature and Volume Fraction Variations on the Effective Thermal Conductivity of Nanoparticle Suspensions (Nanofluids), *J. Appl. Phys.*, 99(8), 084314.
- Maxwell J. C., 1873, *A Treatise on Electricity and Magnetism* (Vol.II), Clarendon Press, Oxford, 54.
- Murshed S. M. S., Leong K.C. and Yang C., 2008, Investigations of Thermal Conductivity and Viscosity of Nanofluids, *Int. J. Therm. Sci.*, 47(5), 560-568.
- Murshed S. M. S., Leong K.C. and Yang C., 2009, A Combined Model for the Effective Thermal Conductivity of Nanofluids, *Appl. Therm. Eng.*, 29(11-12), 2477-2483.
- Oztop H. F. and Abu-Nada E., 2008, Numerical Study of Natural Convection in Partially Heated Rectangular Enclosures Filled with Nanofluids, *Int. J. Heat Fluid Flow*, 29(5), 1326-1336.
- Pak B.C. and Cho Y. I., 1998, Hydrodynamic and Heat Transfer Study of Dispersed Fluids with Submicron Metallic Oxide Particles, *Exp. Heat Transfer*, 11(2), 151-170.
- Rahman M. M., Billah M. M., Rahman A. T. M. M., Kalam M. A., Ahsan A., 2011, Numerical Investigation of Heat Transfer Enhancement of Nanofluids in an Inclined Lid-Driven Triangular Enclosure, *Int. Commun. Heat Mass Transfer*, 38(10), 1360-1367.
- Susantez Ç., Kahveci K., Cihan A. and Hacıhafizoğlu O. 2012, Natural Convection of Water-Based CuO Nanofluids in an Enclosure with a Heat Conducting Solid Circular Cylinder at the Center. *6th International Ege Energy Symposium & Exhibition*, İzmir, 653-664.
- Wang X., Xu X. and Choi S. U. S., 1999, Thermal Conductivity of Nanoparticle-Fluid Mixture, *J. Thermophys Heat Transfer*, 13(4), 474-480.
- Wong K. V. and Leon O., 2010, Applications of Nanofluids: Current and Future (Review Article), *Advances in Mechanical Engineering*, 2, 1-11.
- Xuan Y. and Li Q., 2000, Heat Transfer Enhancement of Nanofluids, *Int. J. Heat Fluid Flow*, 21(1), 58-64.
- Xuan Y. and Li Q., 2003, Investigation on Convective Heat Transfer and Flow Features of Nanofluids, *J. Heat Transfer*, 125(1), 151-155.

Yu W., and Choi S. U. S., 2003, The Role of Interfacial Layers in the Enhanced Thermal Conductivity of Nanofluids: A Renovated Maxwell Model, *J. Nanopart. Res.*, 5(1), 167–171.

Yu Z. T., Xu X., Hu Y. C., Fan L. W. and Cen K. F., 2011, Numerical Study of Transient Buoyancy-Driven Convective Heat Transfer of Water-Based Nanofluids in a Bottom-Heated Isosceles Triangular Enclosure, *Int. J. Heat Mass Transfer*, 54(1-3), 526–532.



Çiğdem SUSANTEZ was born in İstanbul-Turkey in 1982. She graduated from the Mechanical Engineering Department of Trakya University in 2007 as a highest ranking student of the department and faculty. She worked as a research assistant between 2009 and 2016. She obtained her PhD degree in 2015 from Trakya University. She has been working as an Assistant Professor at Mechanical Engineering Department of Trakya University since 2016. Her main research fields are heat transfer and fluid mechanics.



Kamil KAHVECİ was born in Bayburt-Turkey in 1971. He graduated from the Mechanical Engineering Department of Trakya University in 1993. He obtained his MSc degree in 1995 and PhD degree in 1998 from Trakya University. He has been working as a Professor at Trakya University since 2015. His main research fields are heat transfer and fluid mechanics.